A HIGHER-ORDER STATISTICS-BASED VIRTUAL INSTRUMENT FOR TERMITE ACTIVITY TARGETING

Juan José González de la Rosa, José Melgar Camarero, Stephane Bouaud, J. G. Ramiro
Univ. Cádiz, Electronics Area, Research Group PAI-TIC-168, EPSA, Av. Ramón Puyol S/N, E-11202-Algeciras-Cádiz, Spain
juanjose.delarosa@uca.es

Antonio Moreno Muñoz
Univ. Córdoba. Electronics Area. Research Group PAI-TIC-168
Campus Rabanales, A. Einstein C-2, E-14071, Córdoba, Spain
amoreno@uco.es

Keywords: Acoustic Emission, Discrete Wavelet Transform, Higher-Order Statistics, Insect detection, Spectral kurtosis, Transient detection.

Abstract: In this paper we present the operation results of a portable computer-based measurement equipment conceived to perform non-destructive testing of suspicious termite infestations. Its signal processing module is based in the spectral kurtosis (SK), with the de-noising complement of the discrete wavelet transform (DWT). The SK pattern allows the targeting of alarms and activity signals. The DWT complements the SK, by keeping the successive approximations of the termite emissions, supposed more non-gaussian (less noisy) and with less entropy than the detail approximations. For a given mother wavelet, the maximum acceptable level, in the wavelet decomposition tree, which preserves the insects' emissions features, depends on the comparative evolution of the approximations details' entropies, and the value of the global spectral kurtosis associated to the approximation of the separated signals. The paper explains the detection criterion by showing different types of real-life recordings (alarms, activity, and background).

1 INTRODUCTION

Biological transients gather all the natural complexity of their associated sources, and the media through which they propagate. As a consequence, finding the most adequate method to get a complete characterization of the emission, implies the selection of the appropriate model, which better explains the processes of generation, propagation and capture of the emitted signals. This description matches the issue of measurement termite activity.

This paper deals with the performance of a final-version equipment (computer-based signal processing unit), whose previous prototype's performance, based in the time-frequency domain analysis of the kurtosis, was described in (De la Rosa and Muñoz, 2008,). In this final version, the measurement method is mainly based in the interpretation of the spectral kurtosis graph, along with the wavelet analysis, which is thought as an aid. At the same time, we use a simple data acquisition unit, the sound card (maximum speed at 44,100 Hz), which simplifies the hardware unit and the criterion of detection.

The instruments for plague detection are thought with the objective of decreasing subjectiveness of the field operator. On-site monitoring implies reproducing the natural phenomenon of insect emissions with high accuracy. As a consequence it is imperative the use of a deep storage device, and high sensitive probes with selective frequency characteristics. These features make the price paid very high, and still do not guarantee the success of the detection. Besides, the expert's subjectiveness plays a crucial role, because only trained field operators can separate the signals of interest from the non-usable background.

Regarding the procedures, the methods in which the instruments are based are very much dependent on the detection of excess of power in the signals; these are the so-called second-order methods. For example, the RMS calculation can only characterize the intensity (amplitude level of the signal), and does not provide information regarding the envelope of the signal nor the time fluctuations of the amplitude. Another handicap of the second-order principle, e.g. the classical power spectrum, attends to the preservation of the energy during data processing. Consequently, the eradication of additive noise lies in filter design and sub-band decomposition, like wavelets and wavelet

packets.

As an alternative to improve noise rejection and complete characterization of the signals, in the past ten years, a myriad of higher-order methods are being applied in different fields of Science and Technology, in scenarios which involve signal separation and characterization of non-Gaussian signals. Concretely, the area of diagnostics-monitoring of rotating machines is also under our interest due to the similarities of the signals to be monitored with the transients from termites. Many time-series of faulty rotating machines consist of more-or-less repetitive short transients of random amplitudes and random occurrences of the impulses.

This paper describes a method based in the spectral kurtosis (related to the fourth-order cumulant at zero lags) to detect infestations of subterranean termites in a real-life scenario (southern Spain). Wavelet decomposition is used as an extra tool to aid detection from the preservation of the approximation of the signal, which is thought to be more Gaussian than the details.

The interpretation of the results is focussed on the classical peakedness of the statistical probability distribution associated to each frequency component of the signal, to get a measure of the distance from the Gaussian distribution. The spectral kurtosis serves as a twofold tool. First, it enhances non-Gaussian signals over the background. Secondly, it offers a more complete characterization of the transients emitted by the insects, providing the user with the probability associated to each frequency component.

The paper is structured as follows: in Section 2 a review on termite detection and relevant HOS experiences sets the foundations. In Section 3 we make a brief report on the definition of kurtosis; we use an unbiased estimator of the spectral kurtosis, successfully used in (De la Rosa and Muñoz, 2008,), using a higher measurement bandwidth. Results are presented in Section 5. Finally, conclusions are drawn in Section 6.

2 TERMITE DETECTION AND HIGHER-ORDER STATISTICS

2.1 Subterranean Termites: Fundamentals

Termites have become a threat in all the modern countries, mainly due to the advent of central heating in the buildings. Cause more damage to homes in U.S.A. than storms and fire combined, on the average, there could be as many as 15 to 20 subterranean termite colonies per hectare, which means that for example a typical U.S.A. home may easily have three to four colonies situated under or around it. Colonies can contain up to 1,000,000 members (De la Rosa and Muñoz, 2008,).

Termite detection has been gaining importance within the research community in the last two decades, mainly due to the urgent necessity of avoiding the use of harming termiticides, and to the joint use of new emerging techniques of detection and hormonal treatments (IGR[1] products), with the aim of performing an early treatment of the infestation. A localized partial infestation can be exterminated after two or three generations of the colony's members with the aid of these hormones, which stop chitin synthesis. A chitin synthesis inhibitor kills termites by inhibiting formation of a new exoskeleton when they shed their existing exoskeleton. As a direct consequence, the weakened unprotected *workers* stop feeding the *queen* termite of the colony, which dies of starvation, finishing the reproduction process, and consequently cutting any possible replacement of the members of the colony with a new generation. In this paper the specie *reticulitermes lucifugus* is under study.

2.2 Subterranean Termites: Detection Project towards HOS

The primary method of termite detection consists of looking for evidence of activity. But only about 25 percent of the building structure is accessible, and the conclusions depend very much on the level of expertise and the criteria of the inspector (De la Rosa and Muñoz, 2008,),(Robbins et al., 1991). As a consequence, new techniques have been developed to remove subjectiveness and gain accessibility.

User-friendly equipment is being currently used in targeting subterranean insect infestations by means of temporal analysis of the vibratory data sequences [2]. An acoustic-emission (AE) sensor or an accelerometer is fixed to the suspicious structure. This class of instruments is based on the calculation of the root mean square (RMS) value of the vibratory waveform. The RMS value comprises information of the AE raw signal power during each time-interval of measurement (averaging time). This measurement strategy conveys a loss of potentially valuable information both in the time and in the frequency domain (De la Rosa and Muñoz, 2008,).

[1] **I**nhibitor **G**rowth **R**egulators

[2] The system AED2000 (Acoustic Emission Consulting) has proven to be an advance in the detection of several insect species.

On the other hand, the use of the RMS value can be justified both by the difficulty of working with raw AE signals in the high-frequency range, and the scarce information about sources and propagation properties of the AE waves through the substratum. Noisy media and anisotropy makes even harder the implementation of new methods of calculation and measurement procedures. A more sophisticated family of instruments makes use of spectral analysis and digital filtering to detect and characterize vibratory signals (Mankin and Fisher, 2002).

Other complementary second-order tools, like wavelets and wavelet packets (time-dependent technique) concentrate on transients and non-stationary movements, making possible the detection of singularities and sharp transitions, by means of sub-band decomposition. The method has been proved under controlled laboratory conditions, up to a SNR=-30 dB (De la Rosa et al., 2006,).

Higher-order statistics, are being widely used in several fields. The following are relevant due to the similarities of the problems they study. The spectral kurtosis has been successfully described and applied to the vibratory surveillance and diagnostics of rotating machines (Antoni, 2006a),(Antoni, 2006b), showing an inedit set of results that include kurtogram-based calculations of optimal band-pass filters and their performance in detecting two types of machinery faults (ball faults and outer race fault in rolling elements bearings); the kurtosis of the filtered signals is enhanced, which improves the detection of the fault type under study.

In the field of insect detection, the work presented in (De la Rosa and Muñoz, 2008,) set the foundations of the present paper. The combined used of the spectral kurtosis and the time-domain sliding kurtosis showed marked features associated to termite emissions. In the frequency domain (sample frequency 64,000 Hz) three frequency zones were identified in the spectral kurtosis graph as evidence of infestation; two in the audio band (which will be also checked in the present paper) and one in the near ultrasound ($\approx$ 22 kHz). In the present paper the sample frequency was fixed to 44,100 Hz and the sound card was directly driven by MATLAB, which presents the results in an user-oriented interface, which is forwarded in Fig. 1. In the measurement situation shown in Fig. 1, the time-raw data contains alarms an activity signals from termites. This is a clear example of positive detection.

The developed virtual instrument also calculates and presents the spectrum (up-right graph) and the raw data (bottom-left). The field operator adds therefore visual information to the classical audio-based

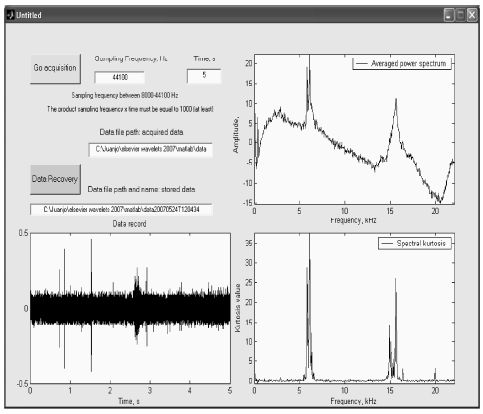

Figure 1: The graphical user interface which presents the results to the field operator. The spectral kurtosis is in the bottom-right corner.

criterion, which was by the way very subjective and very expertise-depend.

Other relevant achievements related to HOS are the following. Cumulants have been modeled in order to characterize the ultrasound waves in materials (Miralles et al., 2004). Bi-cepstrum, have been successfully used in blind identification of acoustic emissions (Iturrospe et al., 2005). Bi-spectrum has been applied to enhance reflections in ring-type samples of steel pipes, in a non-destructive testing frame (De la Rosa et al., 2007b,).

In the field of termite detection, a cumulant-based independent component analysis algorithm has proven to separate termites' alarm signals from synthetics noise backgrounds (De la Rosa et al., 2005,) in a blind source separation scenario. The information contained in the diagonal of the bi-spectrum data structure has proven to enhance the frequency pattern of the termites' emissions (De la Rosa et al., 2007a,). The conclusions of these works were funded in the advantages of cumulants; in particular, in the capability of enhancing the SNR of a signal buried in noise processes, whose probability dnsity function is symmetrically distributed. The computational cost (memory consuming) could be pointed as the main drawback of the technique. Calculation of the cumulants' is made for all the combinations of time lags, giving rise to complex multidimensional data structures. The exam of this data sets leads to the selection of a privileged direction, whose which data are analyzed. In this paper, time-lags are set to zero in order to reduce the cost of computation. Statistically speaking, zero time lags lead to kurtosis, in a fourth-order cumulant.

3 KURTOSIS AND SPECTRAL KURTOSIS

3.1 Kurtosis, *4*th-order Cumulants and its Interpretation

Kurtosis is a measure of the "peakedness" of the probability distribution of a real-valued random variable. Higher kurtosis means more of the variance is due to infrequent extreme deviations, as opposed to frequent modestly-sized deviations. This fact is by the way used in this paper to detect termite emissions in an urban background. Kurtosis is more commonly defined as the fourth central cumulant divided by the square of the variance of the probability distribution, which is the so-called excess kurtosis:

$$\gamma_2 = \frac{\kappa_4}{\kappa_2^2} = \frac{\mu_4}{\sigma^4} - 3, \tag{1}$$

where $\mu_4 = \kappa_4 + 3\kappa_2^2$ is the *4*th-order central moment; and κ_4 is the *4*th-order central cumulant, i.d. the ideal value of $Cum_{4,x}(0,0,0)$. This definition of the *4*th-order cumulant for zero time-lags comes from a combinational relationship among the cumulants of stochastic signals and their moments, and is given by the *Leonov-Shiryaev* formula. A complete description for these statistics are found for example in (Nikias and Mendel, 1993; Mendel, 1991; Chonavel, 2003).

The "minus 3" at the end of this formula is a correction to make the kurtosis of the normal distribution equal to zero. Excess kurtosis can range from -2 to $+\infty$.

The sample kurtosis is calculated over a sample-register (an *N*-point data record), and noted by:

$$g_2 = \frac{m_4}{s^4} - 3 = \frac{m_4}{m_2^2} - 3 = \frac{\frac{1}{N}\sum_{i=1}^{N}(x_i - \bar{x})^4}{\frac{1}{N^2}\left[\sum_{i=1}^{N}(x_i - \bar{x})^2\right]^2} - 3, \tag{2}$$

where m_4 is the fourth sample moment about the mean, m_2 is the second sample moment about the mean (that is, the sample variance), and $\bar{x}$ is the sample mean. The sample kurtosis defined in Eq. (2) is a biased estimator of the population kurtosis, if we consider a sub-set of samples from the population (the observed data).

3.2 Spectral Kurtosis Estimation and Interpretation

Ideally, the spectral kurtosis is a representation of the kurtosis of each frequency component of a process (or data from a measurement instrument x_i). For estimation issues we will consider M realizations of the process; each realization containing N points; i.d. we consider M measurement sweeps, each sweep with N points. The time spacing between points is the sampling period, T_s, of the data acquisition unit.

A biased estimator for the spectral kurtosis for a number M of *N*-point realizations at the frequency index m, is given by:

$$\hat{G}_{2,X}^{N,M}(m) = \\ = \frac{M}{M-1}\left[\frac{(M+1)\sum_{i=1}^{M}|X_N^i(m)|^4}{\left(\sum_{i=1}^{M}|X_N^i(m)|^2\right)^2} - 2\right]. \tag{3}$$

This estimator is the one we have implemented in the program code in order to perform the data computation and it was also used successfully in (Vrabie et al., 2003; De la Rosa and Muñoz, 2008,).

Regarding the experimental signals, we expect to detect positive peaks in the kurtosis's spectrum, which may be associated to termite emissions, characterized by random-amplitude impulse-like events. This non-Gaussian behavior should be enhanced over the symmetrically distributed electronic noise, introduced in the measurement system. Speech is perhaps also reflected in the spectral kurtosis but not in the frequencies were termite emissions manifest. Besides, we assume, as a starting point, that non-Gaussian behavior of termite emissions is more acute than in speech. As a consequence, these emissions would be clearly outlined in the kurtosis spectrum. As a final remark, we expect that constant amplitude interferences are clearly differentiate due to their negative peaks in the spectral kurtosis. To show the ideal performance of the estimator, which has been described in these lines, and also described in (De la Rosa and Muñoz, 2008,), we show an example based in synthetics. A mix of six different signals have been designed. Each mixture is the sum of a constant-amplitude sine of 2 kHz, a constant-amplitude sine at 9 kHz, a Gaussian-distributed-amplitude sine al 5 kHz, a Gaussian-distributed-amplitude sine at 18 kHz, a Gaussian white noise, and a colored Gaussian noise between 12 and 13 kHz. Each mixture (realization or sample register) contains 1324 points.

Negative kurtosis is expected for constant-amplitude processes, positive kurtosis should be associated to random-amplitudes and zero kurtosis will characterize both Gaussian-noise processes.

A simulation has been made in order to show the influence of the number of sample registers (M) in the averaged results for the SK graph. Fig. 2 shows a good performance because enough registers have

been averaged (M=500). For M ¡ 100, roughly, performance degenerates.

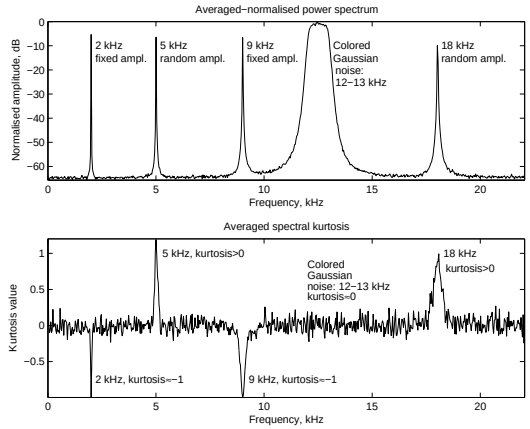

Figure 2: Performance over a set of synthetics, for M=500 realizations.

Once we have expose the main criterion used by the instrument, we make a brief recall of wavelets transforms, which are used as a complement in the following way. First of all, they manage to extract the impulses buried in noise and other parasitic signals. Secondly, the successive approximations of the signals, in the wavelet decomposition tree are supposed to gather all the non-Gaussian features or components, while the details are mainly composed by random signals, with a high entropy. So, the global SK (averaged SK, over all the frequency components) will be higher as the decomposition level increases.

4 THE WAVELET TRANSFORM DECOMPOSITION: FUNDAMENTALS AND DECISION CRITERIA

A *mother wavelet* is a function ψ with finite energy[3], and zero average:

$$\int_{-\infty}^{+\infty} \psi(t)dt = 0, \tag{4}$$

This function is normalized[4], $\|\psi\| = 1$, and is centered in the neighborhood of t=0.

$\psi(t)$ can be expanded with a scale parameter a, and translated by b, resulting the *daughter functions* or *wavelet atoms*, which remain normalized:

$$\psi_{a,b}(t) = \frac{1}{\sqrt{a}}\psi\left(\frac{t-b}{a}\right); \tag{5}$$

The CWT can be considered as a correlation between the signal under study $s(t)$ and the wavelets (*daughters*). For a real signal $s(t)$, the definition of CWT is:

$$CWTs(a,b) = \frac{1}{\sqrt{a}}\int_{-\infty}^{+\infty} s(t)\psi^*\left(\frac{t-b}{a}\right)dt; \tag{6}$$

where $\psi^*(t)$ is the complex conjugate of the mother wavelet $\psi(t)$, $s(t)$ is the signal under study, and a and b are the scale and the position respectively ($a \in \Re^+ - 0, b \in \Re$). The scale parameter is proportional to the reciprocal of the frequency. Eq. (6) establishes that each coefficient provide numerical information about the similarity between the signal under study and the time-shifted frequency-scaled wavelet daughter.

The Discrete Time Wavelet Transform (DTWT) is introduced in order to to reduce the computational cost of calculating all these coefficients. Only a subset of scale and time shifts are chosen in the DTWT. A tree-structure arrangement of filters allows the subband decomposition of the signal. The original signal passes through two complementary filters (*quadrature mirror filters*), and two signals are obtained as a result of a down-sampling process, corresponding to the approximation and detail coefficients.

The lengths of the detail and approximation coefficient vectors are slightly more than half the length of the original signal, $s(t)$. This is the result of the digital filtering process (convolution) (Angrisani et al., 1999). The approximations are the high-scale, low-frequency components of the signal. The details are the low-scale, high-frequency components.

Daubechies 5 has been selected as most similar wavelet mother, because of the highest coefficients in the decomposition tree. Given the wavelet mother, to show the process of selecting the maximum decomposition level in the wavelet tree, we have adopted a criterion based on the calculation of Shannon's entropy (information entropy), which is a measure of the uncertainty associated with a random variable X; this entropy denoted by $H(X)$, and defined by:

$$H(X) := -\sum_{i=1}^{N} p(x_i)\log_{10} p(x_i), \tag{7}$$

where X is an N-outcome measurement process $\{x_i, i = 1, \cdots, N\}$, and $p(x_i)$ is the probability density function of the outcome x_i.

We show this strategy via the following example, based on real-life data, presented in Fig. 6 and in Fig.

[3] $f \in \mathbf{L}^2(\Re)$, the space of the finite energy functions, verifying $\int_{-\infty}^{+\infty} |f(t)|^2\, dt < +\infty$.

[4] $\|f\| = \left(\int_{-\infty}^{+\infty} |f(t)|^2\, dt\right)^{1/2} = 1$.

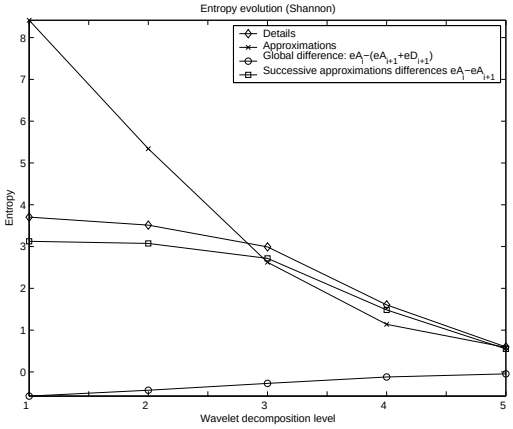

Figure 3: Evolution of the entropy.

7, in the results section. The entropy of the approximations and the details are compared for each level of comparison and shown in Fig. 3.

By looking at the graph of Fig. 3, at level 4, the entropy of the approximations is less than the entropy of the details. So level 4 is in a sense, a point of inversion. No improvement is obtained for level 5, where the entropies are very similar.

We can also see that the global difference of entropies increases towards zero, at level 5, as a complementary indication that further decomposition will not suppose progress in de-noising.

5 EXPERIMENTS AND RESULTS

5.1 The Instrument and the Measurement Procedure

A piezoelectric probe-sensor (model SP-1L from *Acoustic Emission Consulting*) is used in the final version of the instrument, and was described in detail in (De la Rosa and Muñoz, 2008,). The sensor is connected to the sound card of a lap-top computer and the acquisition is driven by MATLAB, via the Graphical User Interface (GUI).

The user interface was presented in Fig. 1. The operator can select the acquisition time and the sample frequency (maximum 44,100 Hz if the sound card is driven). In the bottom-right corner of Fig. 1, the spectral kurtosis graph is presented. The user can also examine the raw data and the spectrum. Automatically, the instrument save the acquired data (labeling the file with the date). Additionally, the operator can recall the stored files.

The transducer SP-1L was used to record the data registers in the field experience, and the ICP unit (**I**ntegrated **C**ircuit **P**iezoelectric; ICP interface) was connected to the sound card of a lap-top computer, configuring an autonomous measurement unit. The sampling frequency was F_s=44,100 Hz for all the registers analyzed in this paper, both in the sliding-cumulant results as in the spectral kurtosis subsection. The recording stage took place in a garden with evidence of infestation and the bare waveguide of the sensor was introduced in the lawn, over the suspicious zone. Termite sounds from feeding are like sharp pops and crackles in the audio output.

The key of the spectral kurtosis detection strategy used in this work lies in the potential enhancement of the non-Gaussian behavior of the emissions. If this happens, i.e. if an increase of the non-Gaussian activity (increase in the kurtosis, peakedness of the probability distribution) is observed-measured in the spectral kurtosis graph, there may be infestation in the surrounding subterranean perimeter, where the transducer is attached.

Termite emissions are non-stationary, so the instrument treats data by ensemble averaging of the sample registers, following the indications in (Bendat and Piersol, 2000) (pp. 463-465). Each spectrum and spectral kurtosis graph presented in this section is the result of averaging the spectra of the sample registers, or realizations. As a final remark, acquired data is normalized according to the norm: $\|s\| = \left(\sum_{i=1}^{N} |s_i|^2\right)^{1/2}$.

5.2 Operating Cases

In this subsection we present the possible situations associated to the measurement cases. We present the signals out of the instrument display in order to be analyzed more precisely. A data acquisition time of 5 seconds and a sample frequency of 44,100 Hz have been selected. So every time the user performs an acquisition (pressing the button ”Go”) 220,500 points are stored. The software-engine is adjusted to calculate the averaged spectral kurtosis (SK) over a set of 220 realizations, each of them containing 1,000 points.

Two couples of data registers have been selected as significant examples, corresponding to typical measurements situations. For a given couple, first we present the results without applying wavelets. Then we explain the information wavelets add.

Fig. 4 presents a clear detection case, characterized by termite activity signals without alarms. Two peaks are clearly enhanced in the SK graph (near 5 kHz, and near 15 kHz).

The de-noised data in the time main are shown in the upper grpah of Fig. 5. Applying the spec-

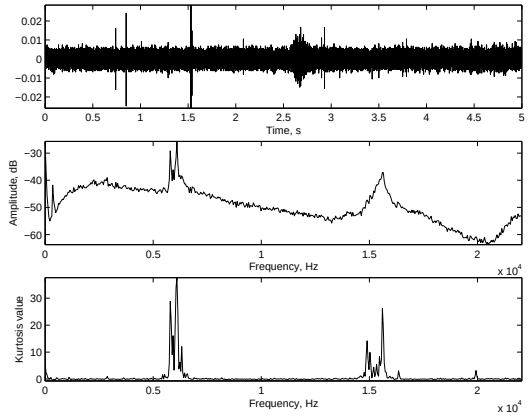

Figure 4: A clear measurement of activity detection.

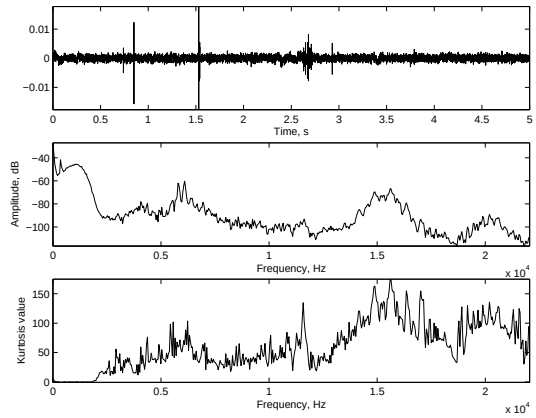

Figure 5: De-noising results for data in Fig. 4. A general enhancement of the spectral kurtosis occurs.

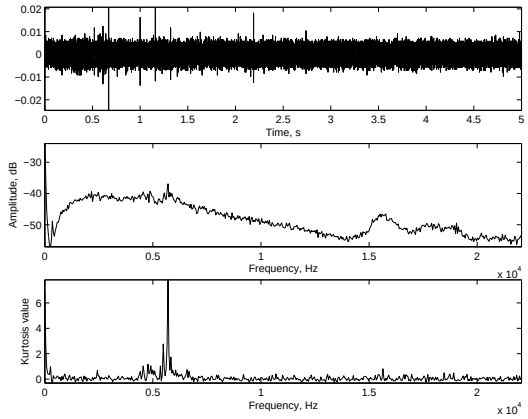

Figure 6: A doubtful measurement situation.

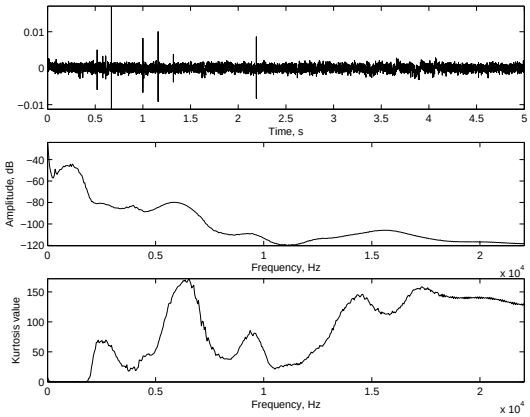

Figure 7: De-noising results of data in Fig. 6.

tral kurtosis to the de-noised version it is seen that all the frequency components are enhanced, specially those ones in the detection band. This fact confirms the presence of insects, and it is of special value in doubtful situations, when they are really needed.

In Fig. 6 a doubtful measurement case is presented. Activity evidence is outlined only near 5 kHz. Once, the wavelets have been applied (shown in Fig. 7), the enhancement near 5 kHz and 15 kHz confirm the detection.

Hereinafter, we present the conclusions.

6 CONCLUSIONS AND ACCOMPLISHMENTS

Assuming the starting hypothesis that the insect emissions may have a more peaked probability distribution than any other simultaneous source of emission in the measurement perimeter, we have design a termite detection strategy and a virtual instrument based in the calculation of the *4*th-order cumulants for zero time lags, which are indicative of the signals' kurtosis. The instrument is actually in use by an Spanish company.

An estimator of the spectral kurtosis has been used to perform a selective analysis of the peakedness of the signal. It has been shown that new frequency components gain in relevance in the spectral kurtosis graphs.

The main goal of this signal-processing method is to reduce subjectiveness due to visual or listening inspection of the registers. This means that in a noisy environment, it may be possible to ignore termite feeding activity even with an *ad hoc* sensor because, despite the fact that the sensor is capable of register these low-level emissions, the human ear can easily ignore them (De la Rosa and Muñoz, 2008,).

ACKNOWLEDGEMENTS

The authors would like to thank the *Spanish Ministry of Science and Education* for funding the project DPI2003-00878, where the different noise processes have been modeled and contrasted; and also for supporting the PETRI project PTR95-0824-OP dealing with plague detection using higher-order statistics. Our unforgettable thanks to the trust we have from the *Andalusian Government* for funding the excellency project PAI2005-TIC00155, where higher-order statistics are modeled and applied to plague detection and power quality analysis.

REFERENCES

Angrisani, L., Daponte, P., and D'Apuzzo, M. (1999). A method for the automatic detection and measurement of transients. part I: the measurement method. *Measurement*, 25(1):19–30.

Antoni, J. (2006a). The spectral kurtosis: a useful tool for characterising non-stationary signals. *Mechanical Systems and Signal Processing (Ed. Elsevier)*, 20(2):282–307.

Antoni, J. (2006b). The spectral kurtosis: application to the vibratory surveillance and diagnostics of rotating machines. *Mechanical Systems and Signal Processing (Ed. Elsevier)*, 20(2):308–331.

Bendat, J. and Piersol, A. (2000). *Random Data Analysis and Measurement Procedures*, volume 1 of *Wiley Series in Probability and Statistics*. Wiley Interscience, 3 edition.

Chonavel, T. (2003). *Statistical Signal Processing. Modelling and Estimation*, volume 1 of *Advanced Textbooks in Control and Signal Processing*. Springer, London, 1 edition.

Iturrospe, A., Dornfeld, D., Atxa, V., and Abete, J. M. (2005). Bicepstrum based blind identification of the acoustic emission (AE) signal in precision turning. *Mechanical Systems and Signal Processing (Ed. Elsevier)*, 19(1):447–466.

Mankin, R. W. and Fisher, J. R. (2002). Current and potential uses of acoustic systems for detection of soil insects infestations. In *Proceedings of the Fourth Symposium on Agroacoustic*, pages 152–158.

Mendel, J. M. (1991). Tutorial on higher-order statistics (spectra) in signal processing and system theory: Theoretical results and some applications. *Proceedings of the IEEE*, 79(3):278–305.

Miralles, R., Vergara, L., and Gosalbez, J. (2004). Material grain noise analysis by using higher-order statistics. *Signal Processing (Ed. Elsevier)*, 84(1):197–205.

Nikias, C. L. and Mendel, J. M. (1993). Signal processing with higher-order spectra. *IEEE Signal Processing Magazine*, pages 10–37.

Robbins, W. P., Mueller, R. K., Schaal, T., and Ebeling, T. (1991). Characteristics of acoustic emission signals generated by termite activity in wood. In *Proceedings of the IEEE Ultrasonic Symposium*, pages 1047–1051.

De la Rosa, J. J. G., Lloret, I., Moreno, A., Puntonet, C. G., and Górriz, J. M. (2006). Wavelets and wavelet packets applied to detect and characterize transient alarm signals from termites. *Measurement (Ed. Elsevier)*, 39(6):553–564. Available online 10 January 2006.

De la Rosa, J. J. G., Lloret, I., Puntonet, C. G., Piotrkowski, R., and Moreno, A. (2007a). Higher-order spectra measurement techniques of termite emissions. a characterization framework. *Measurement (Ed. Elsevier)*, In Press:–. Available online 13 October 2006.

De la Rosa, J. J. G. and Muñoz, A. M. (2008). Higher-order cumulants and spectral kurtosis for early detection of subterranean termites. *Mechanical Systems and Signal Processing (Ed. Elsevier)*, 22(Issue 1):279–294. Available online 1 September 2007.

De la Rosa, J. J. G., Piotrkowski, R., and Ruzzante, J. (2007b). Third-order spectral characterization of acoustic emission signals in ring-type samples from steel pipes for the oil industry. *Mechanical Systems and Signal Processing (Ed. Elsevier)*, 21(Issue 4):1917–1926. Available online 10 October 2006.

De la Rosa, J. J. G., Puntonet, C. G., and Lloret, I. (2005). An application of the independent component analysis to monitor acoustic emission signals generated by termite activity in wood. *Measurement (Ed. Elsevier)*, 37(1):63–76. Available online 12 October 2004.

Vrabie, V., Granjon, P., and Serviere, C. (2003). Spectral kurtosis: from definition to application. In IEEE, editor, *IEEE-EURASIP International Workshop on Nonlinear Signal and Image Processing (NSIP'2003)*, volume 1, pages 1–5.